



RESEARCH ARTICLE

Preparation and characterization of spray deposited TiO₂ thin film as role of solution molarity**Arunachalam Arjunan*, & Ananthi Thanga Thamizh Sithan***Department of Physics, Sri Vinayaga College of Arts & Science, Ulundurpet, Tamilnadu, India.***ARTICLE HISTROY**

Received 02 February 2024

Revised 18 February 2024

Accepted 29 February 2024

Keywords*TiO₂ thin films**Spray pyrolysis**XRD**AFM**HRTEM***ABSTRACT**

The TiO₂ thin films were deposited at the substrate temperatures (450°C) onto glass substrates by spray pyrolysis technique and annealed at 500°C in air. The films were characterized by different techniques to analyze its structural and morphological analyses showed that the films had a polycrystalline tetragonal structure and the surfaces of films consisted of nano-sized particles. (HRTEM) depicts the particle size was noticed. The decrease in the energy band gap with the increase in the grain size is observed. The optical constants (refractive index, extinction coefficient,) were calculated from transmission spectra. The violet and blue emission has been observed from PL spectrum. This study indicates that the properties of TiO₂ thin films could be changed with solution molarity and these films can be used in many technological applications. Also, it is aimed to deposit TiO₂ films with preferential orientation along the c-axis and to study the dye sensitized solar cell.

✉ Arunachalam Arjunan
mailto:arunachalam88@gmail.com

©2024 The Author(s). Published by Panainool Ltd.

Introduction

Among various II-VI semiconductor materials, titanium oxide is one of the important semiconducting metal oxide because it has higher electron mobility at room temperature, has wide band gap energy of 3.7 eV, n-type conductivity, abundant in nature and environmental friendly. TiO₂ thin films are excellent materials in many applications such as in the field of sensors, antireflection coatings. Interfertility filters, solar cells, photocatalysts etc., (Deshmukh et al., 2006; Mardare et al., 2010). With increasing concerns about energy demands and the global warming, the development of low cost and accessible, the

renewable energy production has received substantial attention. Solar power is the most notable among renewable energy resources because of its low environmental impact and global availability. Among alternative forms, the solar cell fabrication using TiO₂, ZnO, SnO₂ semiconductors were researched (Lin et al., 2012; Meen et al., 2012; Wang et al., 2013) are widely fabricated throughout. Among these semiconductor materials, in the field of solar cell fabrication, TiO₂ have been researched widely. Because, TiO₂ is having large band gap (3.7eV) with interesting chemical, electrical and optical

properties with three different crystalline structure: rutile (tetragonal), anatase (tetragonal) and brookite (orthorhombic). Also, its specific properties such as high transparency at UV-Vis region, high refractive index, stability of the chemical composition are the few reasons for the TiO₂ films to be used in the fabrication of solar cells (Bandara et al., 2011; B. Liu et al., 2017). A number of methods have reported for the preparation of TiO₂ thin films, including sol-gel (Vishwas et al., 2009), chemical bath deposition method (Orizu et al., 2023) and spray technique (Raut et al., 2011). Among these, the spray pyrolysis technique is one of the most commonly used techniques for preparation of transparent and conducting oxides owing to its simplicity, non-vacuum system of deposition, and inexpensive method. It can be easily modified for production and device quality oxide films can be obtained over a large area coating.

Among these types, spray technique is easy method for preparing large area, low cost, simplicity. In this method, the high quality films are produced in short duration. The main advantage of this method is uniform coating with the specific composition of the solution, good adhesion and morphology of the film. In the present study, it is aimed to enhance the optical and electrical of TiO₂ using spray pyrolysis method for photovoltaic applications and yield high dye sensitized solar cell.

Materials and Methods

TiO₂ films were deposited at different molarity of precursor concentration (Ts= 0.05, 0.1 and 0.15M) and optimized substrate temperature (Ts = 450°C) using spray pyrolysis technique. The precursor of titanium was titanium acetylacetonate (TiC₁₀H₁₄O₅) (0.1M) was dissolved in ethanol and sprayed onto microscopic glass substrates with dimensions of 75×25 mm². Before preparation of films, glass substrates were well cleaned with water bath followed by HCl, acetone and finally rinsed with distilled water and allowed to dry in oven. The substrates were pre-heated for sufficient time before deposition. In spray unit, the substrate temperature was maintained with the help of

heater by an automatic temperature controller unit to attain the required substrate temperature to an accuracy of $\pm 5^{\circ}\text{C}$. Inside the chamber, the spray head and substrate heater were provided with the exhaust fan through which the hazardous fumes of solutions were driven out. To achieve the uniform coating on the substrate, the spray head was allowed to move in the X-Y plane using microcontroller stepper motor. The spray head could scan an area of 200 × 200 mm with a speed of 20 mm sec⁻¹ and in steps of 5 mm sec⁻¹ at X and Y movement respectively. The spray unit had a control over a flow rate of the precursor solution and over the pressure of the carrier gas. The software is simple and user friendly with minimum required parameters. The parameters that software controlled are X/Y travel, speed, dispensing rate and coating duration. After deposition, the film was allowed to cool slowly at room temperature and washed with distilled water and then dried and annealed at 500°C in air.

Preparation of natural dye

10 g of fresh Hibiscus surattensis flowers was added to 10 ml of alcohol and heated using indirect hydronic heating in boiling water and reflux for 30 min to extract the dye (anthocyanin and chlorophyll). The pure and natural dye solution was obtained by filtering out the solid dregs.

Preparations of counter electrode and electrolyte

The counter electrode used in this paper is cobalt sulphide that acts as a catalyst in redoxing agent the dye. The electrolyte is a key component of all dye-sensitized solar cells (DSSCs). It functions as charge carriers collecting electrons at the cathode and transporting the electrons back to the dye molecules. In terms of cell's efficiency, in this paper electrolyte is the iodide, triiodide (I⁻/I₃⁻) redox couple in an organic matrix, the redox electrolyte consisted 0.3 M LiI (Lithium iodide), 15 mM I₂ (Iodine), 0.5 M PMII (1-propyl-3-methylimidazolium iodide) and 0.2 M polyethylene glycol in acetonitrile.

Fabrication and measurement of DSSC

The TiO_2 film deposited on glass substrates was immersed in dye solution of *Hibiscus Surattensis* for 24 h at room temperature for the dye to absorb properly on the TiO_2 surface and to avoid the rehydration of TiO_2 film. After being dried in hot air oven, the photo electrode was placed on top of the counter electrode (cobalt sulphide) and tightly clipped together to form a cell. A schematic diagram of a DSSC is shown in Fig 1.

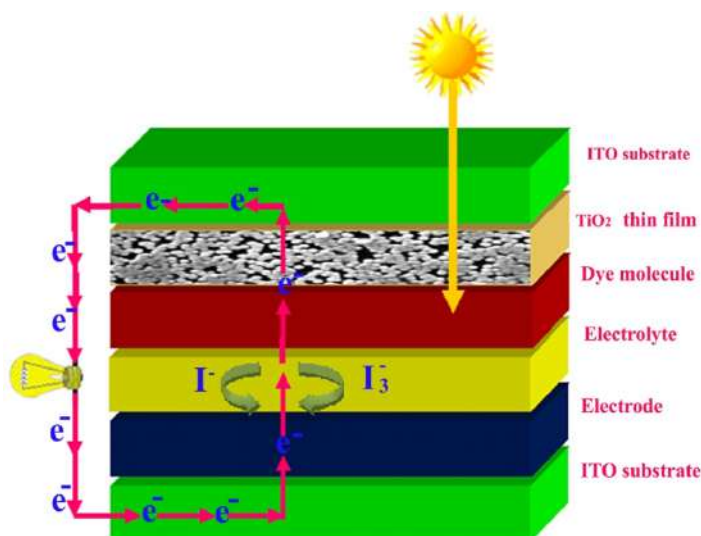


Fig 1. Schematic diagram of DSSC

Working Principle of the DSSC

Dye-sensitized solar cell which is popularly called as DSSC (Fig 2) is a semiconductor device which directly converts the solar radiation into the electric current. The working principle of DSSC was illustrated by (Arunachalam et al., 2015).

1. A transparent anode made up of a glass sheet treated with a transparent conductive oxide layer;
2. A mesoporous oxide layer (typically TiO_2) deposited on the anode to activate electronic conduction.
3. A monolayer charge transfer dye covalently bonded to the surface of the mesoporous oxide layer to enhance light absorption.
4. An electrolyte containing redox mediator in an organic solvent effecting dye-sensitized dye-regenerating and

5. A cathode made of a glass sheet coated with a catalyst (typically, platinum) to facilitate electron collection.

In the performance test of the prepared DSSC, Xenon (Xe) light of 100 W was selected to stimulate sunlight (A.M 1.5), and an I-V analyzer (Keithely 2450) was employed to measure the current against voltage.

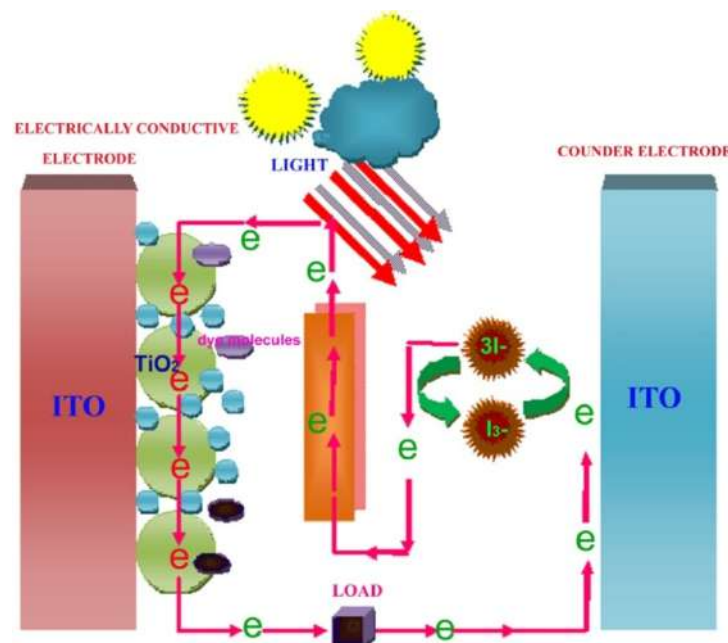


Fig 2. Schematic diagram of working principle of a dye sensitized solar (DSSC)

The structural characterization of the deposited films were carried out by X-ray diffraction technique on SHIMADZU-6000 (monochromatic $\text{Cu-K}\alpha$ radiation, $\lambda=1.5406 \text{ \AA}$). The XRD patterns were recorded in 2θ interval from 10° to 90° with the steps of 0.05° at room temperature. The surface morphology was studied by using SEM (JEOL-JES-1600). The surface topological studies were carried out using Atomic Force Microscope (Nano surf Easy scan2) AGILENT-N9410A-5500. The sample was prepared by placing a small quantity of prepared material on a carbon coated copper grid and allowing the solvent to evaporate, High Resolution Transmission Electron Microscopy (HRTEM), TECNAI G2 FEI F12 model. Optical absorption spectrum was recorded in the range of 300-1200 nm using JASCO V-670 spectrophotometer. The photoluminescence spectrum (PL) was studied at room temperature

using prolog 3-HORIBA|JOBINYVON with an excitation source wavelength of 375 nm. The electrical resistivity, carrier concentration and mobility were measured by an automated Hall Effect measurement (ECOPIA HMS – 2000 version 2.0) at room temperature in a van der Pauw (VDP) four - point probe configuration.

Results and discussion

Structural study

The XRD patterns of the TiO₂ thin films shown for different molar concentrations as shown in the Fig 3. The peak corresponding to (101) plane with low intensity is observed for 0.05M. No systematic peaks were observed at the exact location for any of the crystalline peaks of TiO₂ film. When increasing precursor concentration of 0.1 M the well defined reflections of the films could be indexed in terms of the anatase phase lattice was observed. Whereas at 0.1 M, the major plane (101) with (004), (200), (211) planes of TiO₂ thin film is seen. The pattern of the XRD for the 0.1 M is close with the agreement JCPDS No 21-1272 data for TiO₂ thin films. The films had tetragonal crystal structure and oriented along (101) plane is preferentially oriented along the c-axis which shows the growth tendency of the nano particles in the film. The peak intensities continuously increase with increasing molarity. The increasing film crystallinity can result from more titanium ions in the films. At 0.15 M, the intensity of (101) plane decreases which may be due to structural disorder or reorientation (Nunes et al., 2002). From the above observation the molarity is fixed as (0.1M), and the films are prepared at substrate temperature (Ts = 450°C) to optimize the substrate temperature.

The crystallite size is evaluated from the FWHM of the (101) plane using the Scherrer's formula

$$D = \frac{K\lambda}{\beta \cos \theta} \text{-----1}$$

where K=0.9 is the shape factor, λ is the X-ray wavelength of CuK α radiation, θ is the Bragg's angle and β is the full width at half maximum of the peaks. The lattice strain (ϵ) is calculated using the relation

$$\epsilon = \frac{\beta \cos \theta}{4} \text{-----2}$$

The value of dislocation density (δ) is calculated using the relation

$$\delta = \frac{1}{D^2} \text{-----3}$$

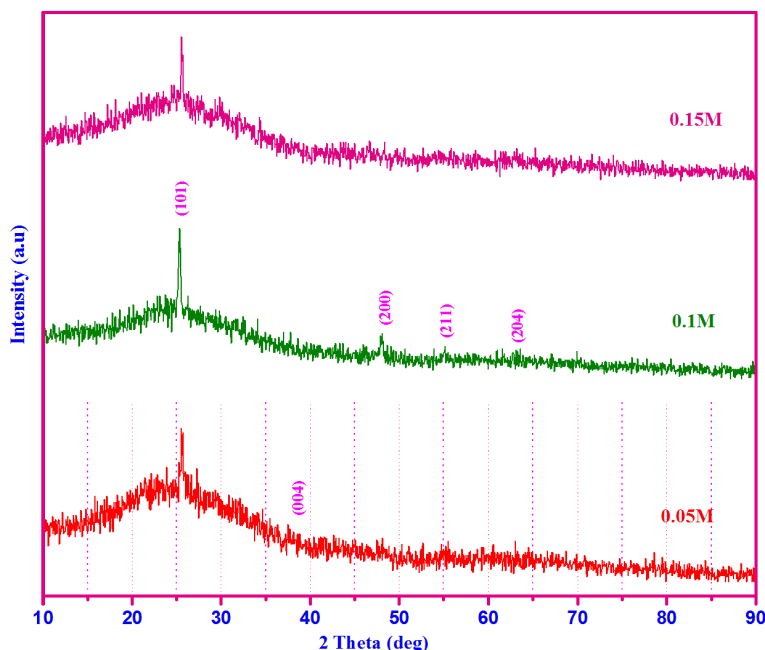


Fig 3. XRD patterns of TiO₂ thin films at different molarities

The structural parameter values were calculated and given in Table 1 the precursor concentration with the crystallite size increased due to particle residence time (Karan et al., 2009). From the Table 1, it is observed that the increase in the crystallite size to decrease in the strain and dislocation density (Fig 4a and b), while both lattice strain and dislocations density decreases (Fig 4a and b). The decrease in strain indicates the decrease in concentration of lattice imperfections, and the formation of high quality film (Vijayalakshmi et al., 2013). The similar result is observed CdO thin films. As seen from these results, it can be said that the crystallinity of films increases with molarity also found that increasing CdO molarity caused an increment in the film crystallinity (Aishwarya et al., 2021; Joishy et al., 2019).

The texture coefficient (TC) represents the texture of a particular plane, deviation of which from unity implies the preferred growth. Quantitative

information concerning the preferential crystallite orientation was obtained from the different texture coefficient $TC_{(hkl)}$ defined as

$$TC_{(hkl)} = \frac{\frac{I_{(hkl)}}{I_{0(hkl)}}}{\frac{1}{n} \sum \frac{I_{(hkl)}}{I_{0(hkl)}}} \text{-----4}$$

Where $TC_{(hkl)}$ is the texture coefficient, $I_{(hkl)}$ is the XRD intensity and n is number of diffraction peaks considered. $I_{0(hkl)}$ is the intensity of the XRD reference of the randomly oriented grains.

the respective direction. At anatase phase, the $TC_{(hkl)}$ increases, which indicate the preferential growth of crystallites in the direction perpendicular to the (hkl) plane is greater (Mariappan et al., 2012).

Table 1. Micro-structural parameters for TiO_2 films obtained at different molarity.

Molarity	Crystallite Size (nm)	Strain (ϵ) $\times 10^{-4}$	Dislocation density (δ) $\times 10^{14}$ lines/ m^2	Texture coefficient
0.05	15.487	2.201	4.034	0.847
0.1	16.339	2.113	3.718	1.094
0.15	18.863	1.837	2.810	0.907

Morphological studies

Surface morphology

Fig 5 shows the SEM micrographs of the surface of the TiO_2 films deposited at different molarities. At 0.05M (Fig 5b), though the grains are visible, they are smaller in size with compact nature. The TiO_2 thin film prepared at the precursor concentration of at 0.1 M exhibits the grains are visible and are in spherical shape and the continuous coverage of the substrate with spherical shape microcrystal with larger size as shown in Fig 5b. The absence of close packed morphology with the porous nature is observed for the film with 0.1M. This porous nature observed at 0.1M of TiO_2 film is useful in DSSC, as it can absorb more dye molecules (Dhanapandian et al., 2016). A further increase in grain size is observed for the film deposited at molar concentration 0.15M (Fig 5c).

Compositional analysis

The elemental analysis of TiO_2 films with 0.1M (representative sample) precursor concentration has been investigated by EDS spectra is shown in Fig 6. The presence of titanium and oxygen is confirmed from the peaks at 0.4 keV and 4.25 keV and 0.48 keV respectively. The presences of other peaks are due to the glass substrate. The relativity near stiochiometry is revealed from the presence of elements Ti and O with atomic percentage 31.22 and 68.78 respectively.

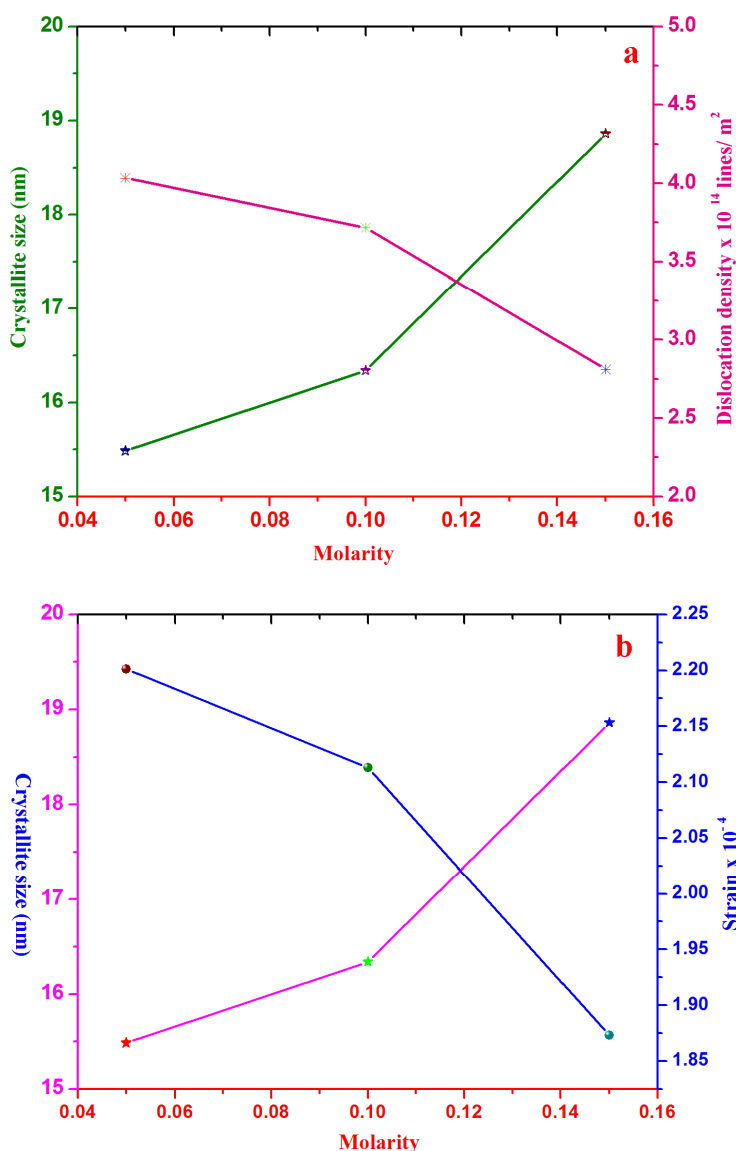


Fig 4 a & b. Crystallite size, Strain and Dislocation density of TiO_2 thin films at different molarities.

From the Table 1, as the molarity increases, the texture coefficient value ranges from $0 < TC_{(hkl)} < 1$ indicates the lack of orientations of the grains in

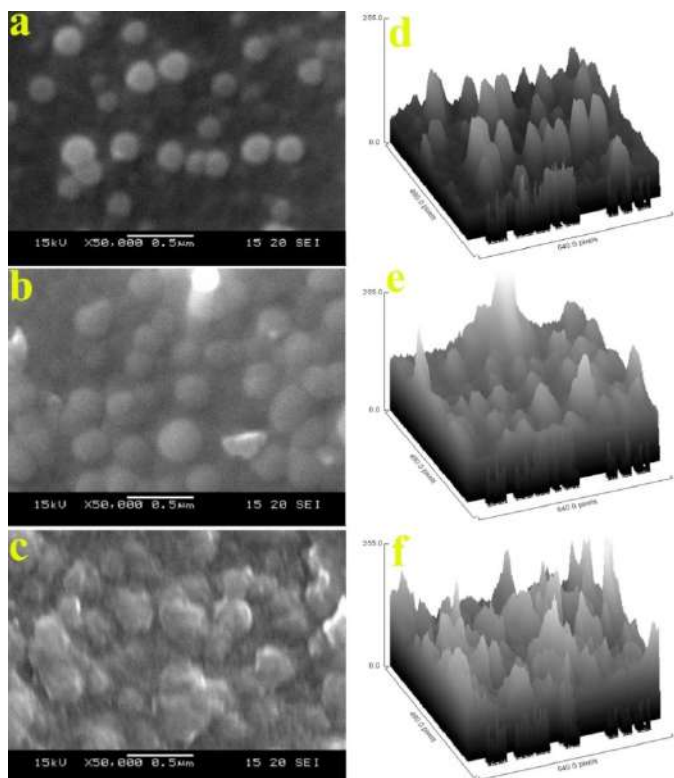


Fig 5. SEM micrograph of TiO_2 thin film a) 0.05M, b) 0.1M, c) 0.15M, d) 0.05M image profile e) 0.1M image profile and f) 0.15M image profile of the selected area of the TiO_2 film.

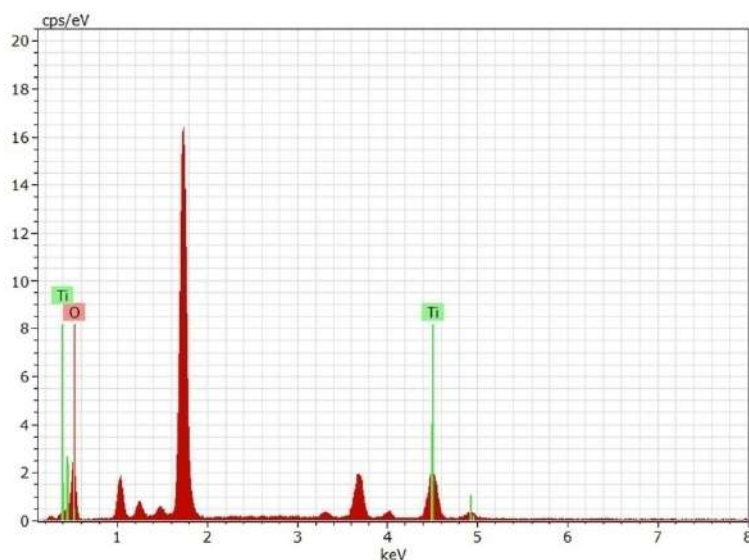


Fig 6. EDX spectrum of the TiO_2 film.

Surface topography

The AFM images of films (Fig 7a, b and c) show that all films consist of nanoparticles and the

particle size continuously increases with increasing molarity, which is in good agreement with the crystallite size variation calculated from XRD results. From Fig 7a, it is evident that in doped film, large clusters/spherical grains ranges from 15 to 25 nm due to the agglomeration of grains with surface roughness 2.3 nm. Fig. 7b represents the topographical image of TiO_2 films deposited at the precursor concentration of 0.1M. The scanned area was $2\ \mu\text{m} \times 2\ \mu\text{m}$. It is clearly observed that the films are uniformly coated without any voids. The films deposited at the optimized temperature exhibited the formation of spherical in shape. Some of the particles possessed hills like structure which grow preferentially along C axis orientation perpendicular to the surface of the substrate. The films deposited at the optimized temperature exhibited the formation porous nature with particle size about 20 nm whereas the particle size of the films at 450°C , are in the range of 15-30 nm respectively. The surface roughness of the films deposited the optimized temperature is 4.4 nm. From the topographical results, it is suggested that the size of the anatase particle is higher also increase in surface roughness are due to increase in molarities. From the morphological and topographical studies, reveals that the film is suitable for the fabrication of DSSC and solar applications (Ngaffo et al., 2007). At higher molar concentration, 0.15 (Fig 7 c), 2D image of the film has a granular morphology with a surface roughness of 7.2 nm.

HRTEM analysis

In the HRTEM image of Fig 8a the TiO_2 thin film structure produced following deposition at 0.1M. The spherical shaped average particle of about 8 nm size is also observed. HRTEM image, shown in the inset of Fig 8a, reveals the determined the Particles present, which confirms the polycrystalline nature of as-prepared nanocrystals. The images show homogeneous with spherical morphology, the spheres consists of many spherical crystals of TiO_2 film is attributed to the agglomeration and histogram indicates narrow size distribution of the particles. Then Fig. 4b is image profile and the selected area diffraction

shown in (Fig 8c) of the TiO_2 film. The size distribution histogram and the films occupied surface volume are given in Fig 8d.

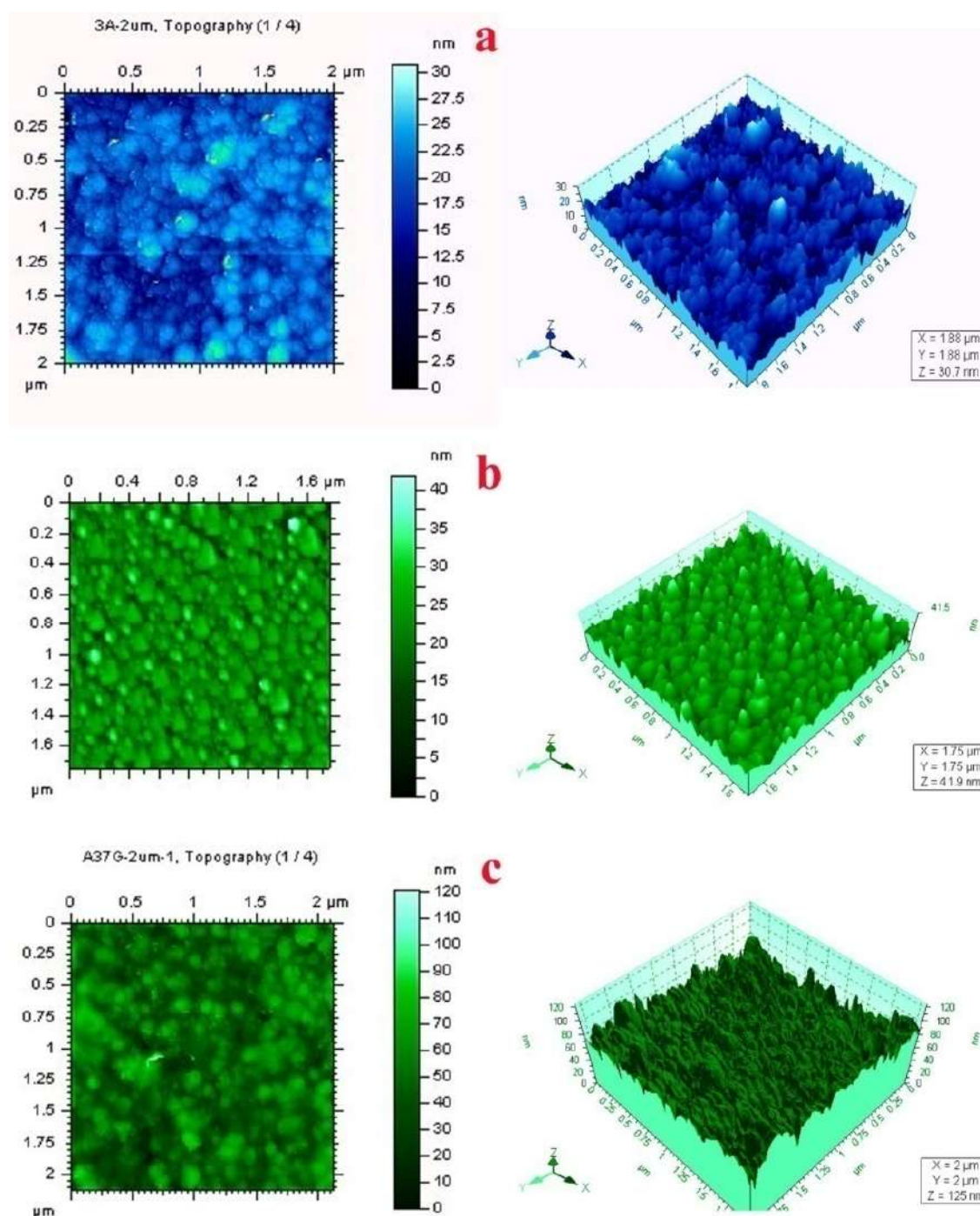


Fig 7. AFM 2D and 3D micrographs of sprayed TiO_2 thin films a) 0.05M, b) 0.1M and c) 0.15M.

Optical Properties

Transmittance

The transmittance spectra for the TiO_2 films deposited at 0.1M molarity of precursor were shown in Fig. 9. The transmittance value was 85%

in the wavelength range of 350 to 1200 nm. At 0.1M molar concentration, the maximum transmittance of enhances up to 85%. This increase in transmittance may be attributed to the well-crystallization of films. The high transparency is associated with a good structural homogeneity

and crystallinity (Shinde et al., 2013). The film with the transmittance higher than 85% is suitable for photovoltaic applications (J. Liu et al., 2012).

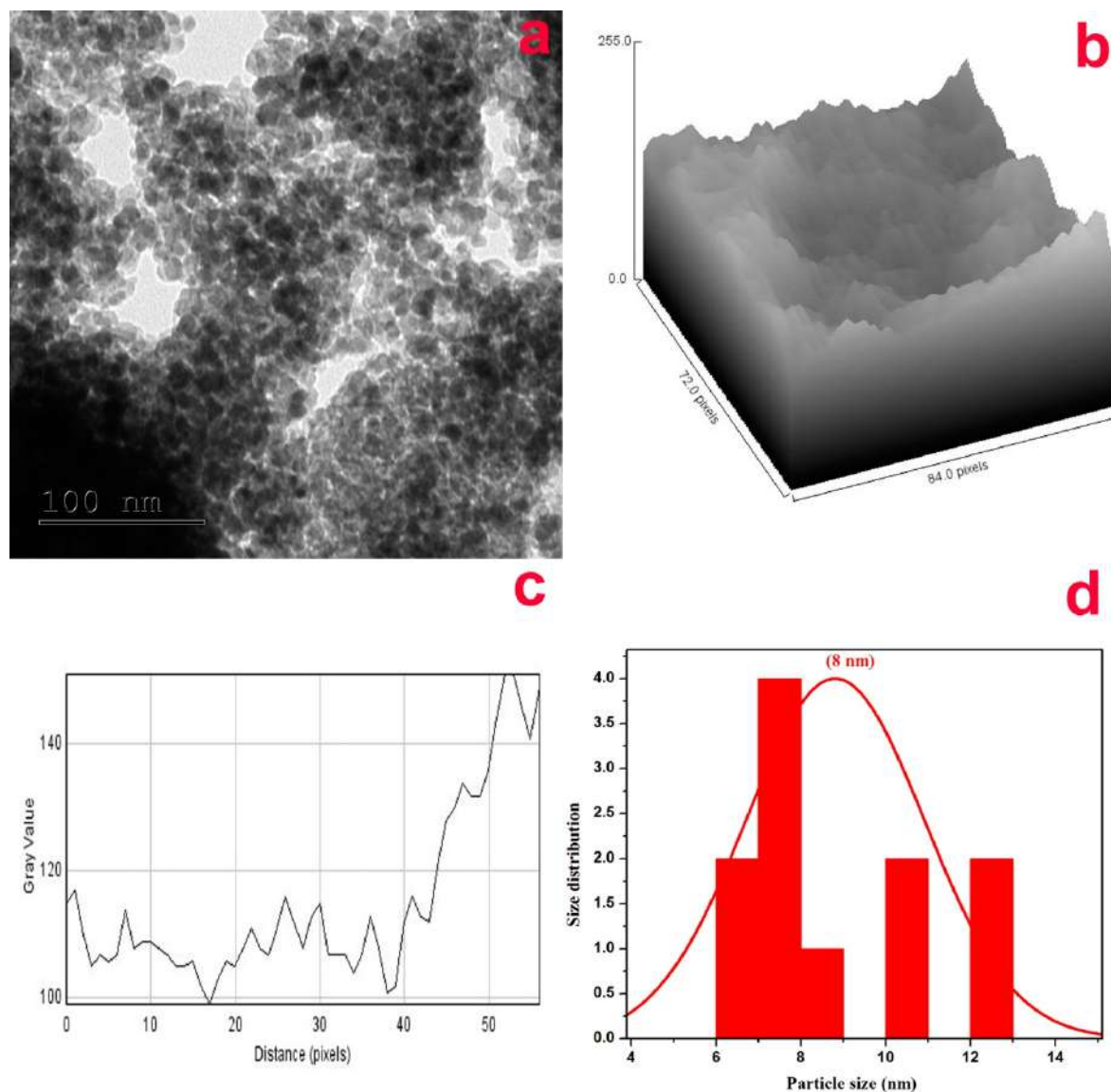


Fig 8. (a) High-resolution transmission electron microscopy (HR-TEM) images of TiO₂ thin film b) surface plot area and (c) Plot profile and particle size selected area highlighted in fig.6a and Average particle size distribution of 8nm TiO₂ thin film in Fig 6d.

Optical band gap

The optical band gap energy E_g was determined by using the relation

$$(\alpha h\nu) = A (h\nu - E_g)^n \text{ -----5}$$

Where E_g is the optical band gap of the films and A is a constant. In Fig 10, the optical band gap decreases from 3.12 to 2.81 eV with increasing molar concentration. This decrease in the band gap

with increasing molar concentration is attributed to a shift in the energy of the valence and conduction bands resulting from electron-impurity and electron-electron scattering. These two effects together decide the change in optical energy band gap (Firdaus et al., 2012).

Extinction coefficient and Refractive index

The extinction coefficient ' k ' and the refractive index ' n ' for titanium dioxide nano thin films with

molarities were determined using the following expression

$$k = \frac{a\lambda}{4\pi} \text{ -----6}$$

decreased as the wavelength increases, which shows the qualitative indication of surface smoothness and homogeneity of the sprayed films (Shanmuganathan et al., 2013).

The refractive index of the film is calculated using

$$n = \frac{1+R^{1/2}}{1-R^{1/2}} \text{ -----7}$$

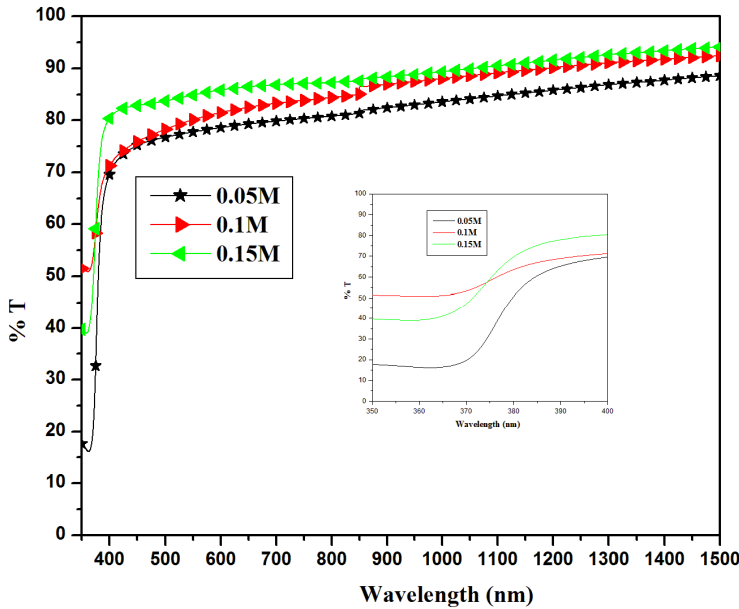


Fig 9. Transmission spectra of sprayed TiO₂ thin films at different molarity and the widened portion of absorption edge (inset).

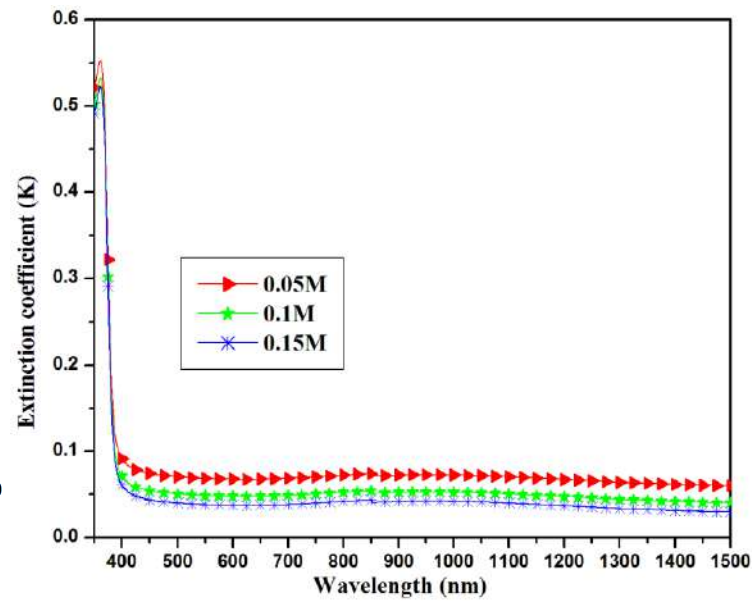


Fig 11. Extinction coefficient (k) of sprayed TiO₂ thin films.

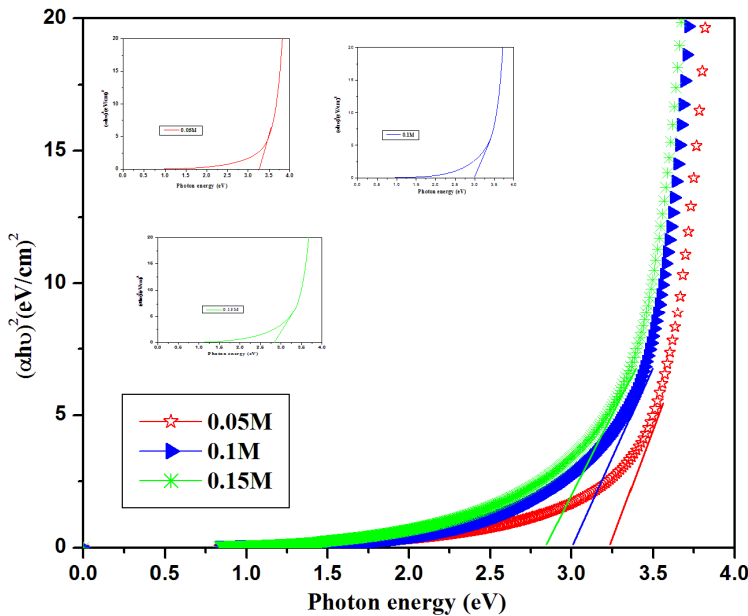


Fig 10. The $(\alpha h\nu)^{1/2}$ vs photon energy plot of the TiO₂ film at different molarity.

The variation in k ranges from 0.1 - 0.55 along the wavelength is shown in Fig 11. The k value

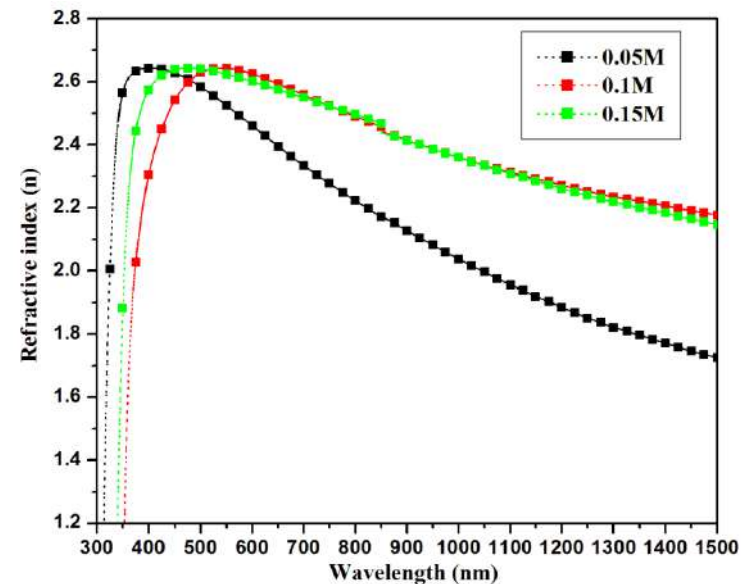


Fig 12. Refractive index (n) of sprayed TiO₂ thin films.

The refractive index plotted against the wavelength is shown in Fig 12. The values of n varies in the range of 1.2-2.64 and is nearly

constant may be due to the variation in temperature. The increase of the refractive index values as a function of the molarity is associated with a densification effect of the deposited films as molarity increases (due to higher surface mobility of the adsorbed species at higher molarity). The refractive index of the doped film shows the variation upto 2.64 in the visible region which is preferred for antireflection coating materials.

Photoluminescence (PL)

The TiO₂ films, exhibits emissions at violet, blue and red are observed in the Fig 13. These emissions are attributed to the band-edge free excitation and bound excitons. The violet emission is probably due to the radiative defects related to the interface traps existing at grain boundaries. The blue emission at 437 nm is due to the transition of electron from the deep donor level of oxygen vacancies to the VB and the electron transition from the deep donor of Ti interstitials to the VB. At 516 nm, the green emission is seen which is associated with the oxygen vacancies and other vacancy related defects (C. Nehru et al., 2012). The peak at 677 nm might be corresponding to the transition from the levels of oxygen interstitial. This oxygen might be occupying the interstitial position giving red emission (Che et al., 2023).

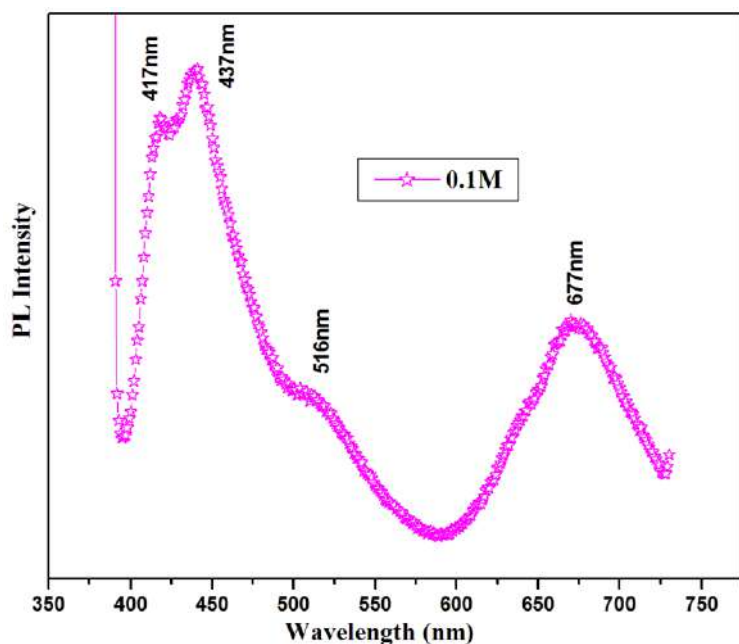


Fig.13. Photoluminescence spectra of the TiO₂ films as a function of molarity.

Electrical Properties

Hall-effect measurements were performed in order to investigate the electrical properties such as, the resistivity, carrier concentration and the Hall-mobility of TiO₂ deposited at 0.1M. The defects such as interstitial Ti atoms and oxygen vacancies can be easily ionized and the electrons induced by this process can contribute to the conduction of electricity, causing TiO₂ to act as an n-type semiconductor. The dependence of resistivity, carrier concentration and mobility on molar concentration is noticed. In the present study, the lowest value of resistivity $3.42 \times 10^2 \Omega \text{ cm}$ with maximum carrier concentration $4.99 \times 10^{21} \text{ cm}^{-3}$ and mobility $0.34 \text{ Cm}^2/\text{Vs}$ is achieved for 0.1M of TiO₂ thin film using the spray pyrolysis technique. The mobility and carrier concentration increases with a decrease in the resistivity which results in the weaker carrier scattering process (Prasada Rao et al., 2010) and this value is agreed well with the reported values in other works employing different techniques.

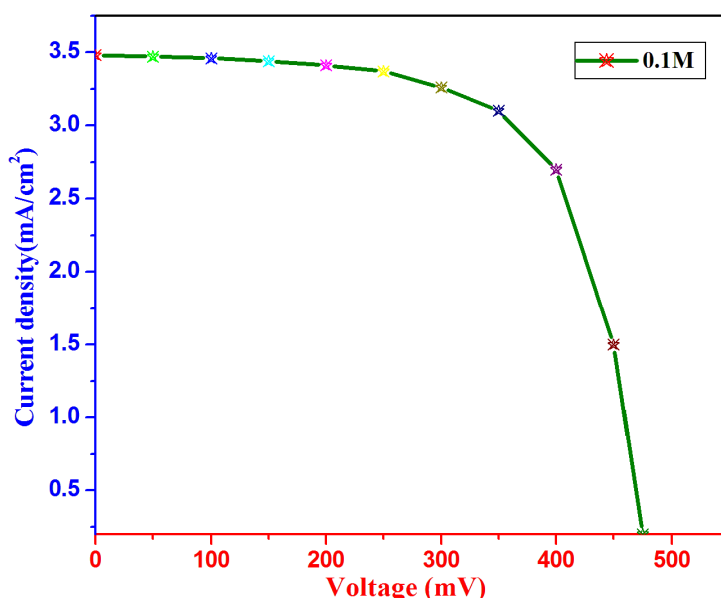


Fig.14. J-V characteristics of DSSC fabricated with 0.1M concentration of TiO₂ photoelectrode with the dye extracted from *Hibiscus surattensis*.

Photovoltaic characterization

Fig 14 shows the photo current voltage (J-V) characteristics of the prepared DSSCs with TiO₂ on

glass substrate deposited at 0.1M concentration as photoelectrode.

The performance parameters of solar cell fabricated with 0.1 Molar concentration with the dye extracted from Hibiscus Surattainsis. From the Fig 14, it is evident that Hibiscus Surattainsis with 0.1concentration of TiO₂ based cell give the best performance with the use of dye as sensitizer reached the maximum value of short-circuit current density, J_{sc} (3.4 mA/cm²), open-circuit voltage, V_{oc} (480 mV), fill-factor, FF (0.81) and efficiency, η (1.5%).

Conclusion

The XRD exposed that at 0.1M with the substrate temperature 450°C, the films exhibited the better crystalline structure with preferentially oriented along (101) plane. With the peak of (101) plane, the formed film was confirmed to be an anatase phase titanium dioxide thin film which is suitable for the preparation of photoelectrode in DSSC. The morphological studies depict the film deposited at 450 C to be in porous nature with nano-sized grains. The surface topography of the film exhibits the tetragonal shaped grains with the particle size of 60 nm and with the increased roughness. The particle size of the TiO₂ film by High Resolution Transmission Electron Microscopy HRTEM was found to be 8 nm. The optical transmittance reached up to 80% with the increase of the band gap. The optical constant, refractive index was higher than the standard value of anatase and therefore it was indicated that it can act as antireflection coating material in DSSC. The emission at 417, 437, 516 and 677 nm were observed. The minimum resistivity was observed for the film deposited at 0.1M. From the antibacterial activity, it is evidenced that the material is determined to the ecosystem. Also the inhibition of bacterial growth and mechanism of antibacterial activity of TiO₂ thin film was highly yielded for the doped film. Therefore, the film prepared with 0.1M at the substrate temperature 450°C is suitable for the preparation of photoelectrode when it is coated on conducting glass plates.

Acknowledgement

The authors thankful to Department of Physics, Sri Vinayaga College of Arts & Science, Ulundurpet, Tamil Nadu, India for carrying out this work.

Conflict of interest

All authors declare that there is no conflict of interest in this work.

References

- Aishwarya, K., Nirmala, R., & Navamathavan, R. (2021). Recent advancements in liquefied petroleum gas sensors: A topical review. *Sensors International*, 2, 100091. <https://doi.org/10.1016/j.sintl.2021.100091>
- Arunachalam, A., Dhanapandian, S., Manoharan, C., & Sridhar, R. (2015). Characterization of sprayed TiO₂ on ITO substrates for solar cell applications. *Spectrochimica Acta Part A: Molecular and Biomolecular Spectroscopy*, 149, 904–912. <https://doi.org/10.1016/j.saa.2015.05.014>
- Bandara, H. M. N., Rajapakse, R. M. G., Murakami, K., Kumara, G. R. R. A., & Anuradha Sepalage, G. (2011). Dye-sensitized solar cell based on optically transparent TiO₂ nanocrystalline electrode prepared by atomized spray pyrolysis technique. *Electrochimica Acta*, 56(25), 9159–9161. <https://doi.org/10.1016/j.electacta.2011.07.119>
- C. Nehru, L., Umadevi, M., & Sanjeeviraja, C. (2012). Studies on Structural, Optical and Electrical Properties of ZnO Thin Films Prepared by the Spray Pyrolysis Method. *International Journal of Materials Engineering*, 2(1), 12–17. <https://doi.org/10.5923/j.ijme.20120201.03>
- Che, L., Song, J., Yang, J., Chen, X., Li, J., Zhang, N., Yang, S., & Wang, Y. (2023). Fluorine, chlorine, and gallium co-doped zinc oxide transparent conductive films fabricated using the sol-gel spin method. *Journal of Materiomics*, 9(4), 745–753. <https://doi.org/https://doi.org/10.1016/j.j>

mat.2023.02.002

- Deshmukh, H. P., Shinde, P. S., & Patil, P. S. (2006). Structural, optical and electrical characterization of spray-deposited TiO₂ thin films. *Materials Science and Engineering: B*, 130(1), 220–227. <https://doi.org/10.1016/j.mseb.2006.03.016>
- Dhanapandian, S., Arunachalam, A., & Manoharan, C. (2016). Highly oriented and physical properties of sprayed anatase Sn-doped TiO₂ thin films with an enhanced antibacterial activity. *Applied Nanoscience*, 6(3), 387–397. <https://doi.org/10.1007/s13204-015-0450-6>
- Firdaus, C. M., Rizam, M. S. B. S., Rusop, M., & Hidayah, S. R. (2012). Characterization of ZnO and ZnO: TiO₂ Thin Films Prepared by Sol-Gel Spray-Spin Coating Technique. *Procedia Engineering*, 41, 1367–1373. <https://doi.org/10.1016/j.proeng.2012.07.323>
- Joishy, S., Kulkarni, S. D., Choudary, R. J., Maidur, S. R., Patil, P. S., & Rajendra, B. V. (2019). Influence of solution molarity on structure, surface morphology, non-linear optical and electric properties of CdO thin films prepared by spray pyrolysis technique. *Materials Research Express*, 6(10), 106447. <https://doi.org/10.1088/2053-1591/ab4153>
- Karan, N. S., Agrawal, A., Pandey, P. K., Smitha, P., Sharma, S. J., Mishra, D. P., & Gajbhiye, N. S. (2009). Diffusion flame synthesis of hollow, anatase TiO₂ nanoparticles. *Materials Science and Engineering: B*, 163(2), 128–133. <https://doi.org/10.1016/j.mseb.2009.05.005>
- Lin, Y.-H., Wu, Y.-C., & Lai, B.-Y. (2012). Collection Efficiency Enhancement of Injected Electrons in Dye-sensitized Solar Cells with a Ti Interfacial Layer and TiCl₄ Treatment. *International Journal of Electrochemical Science*, 7(10), 9478–9487. [https://doi.org/https://doi.org/10.1016/S1452-3981\(23\)16212-2](https://doi.org/https://doi.org/10.1016/S1452-3981(23)16212-2)
- Liu, B., Cheng, K., Nie, S., Zhao, X., Yu, H., Yu, J., Fujishima, A., & Nakata, K. (2017). Ice-Water Quenching Induced Ti³⁺ Self-doped TiO₂ with Surface Lattice Distortion and the Increased Photocatalytic Activity. *The Journal of Physical Chemistry C*, 121(36), 19836–19848. <https://doi.org/10.1021/acs.jpcc.7b06274>
- Liu, J., Ma, S. Y., Huang, X. L., Ma, L. G., Li, F. M., Yang, F. C., Zhao, Q., & Zhang, X. L. (2012). Effects of Ti-doped concentration on the microstructures and optical properties of ZnO thin films. *Superlattices and Microstructures*, 52(4), 765–773. <https://doi.org/10.1016/j.spmi.2012.06.021>
- Mardare, D., Iacomi, F., Cornei, N., Girtan, M., & Luca, D. (2010). Undoped and Cr-doped TiO₂ thin films obtained by spray pyrolysis. *Thin Solid Films*, 518(16), 4586–4589. <https://doi.org/10.1016/j.tsf.2009.12.037>
- Mariappan, R., Ponnuswamy, V., & Suresh, P. (2012). Effect of doping concentration on the structural and optical properties of pure and tin doped zinc oxide thin films by nebulizer spray pyrolysis (NSP) technique. *Superlattices and Microstructures*, 52(3), 500–513. <https://doi.org/https://doi.org/10.1016/j.spmi.2012.05.016>
- Meen, T.-H., Jhuo, Y.-T., Chao, S.-M., Lin, N.-Y., Ji, L.-W., Tsai, J.-K., Wu, T.-C., Chen, W.-R., Water, W., & Huang, C.-J. (2012). Effect of TiO₂ nanotubes with TiCl₄ treatment on the photoelectrode of dye-sensitized solar cells. *Nanoscale Research Letters*, 7(1), 579. <https://doi.org/10.1186/1556-276X-7-579>
- Ngaffo, F. F., Caricato, A. P., Fernandez, M., Martino, M., & Romano, F. (2007). Structural properties of single and multilayer ITO and TiO₂ films deposited by reactive pulsed laser ablation deposition technique. *Applied Surface Science*, 253(15), 6508–6511. <https://doi.org/https://doi.org/10.1016/j.apsusc.2007.01.110>
- Nunes, P., Fortunato, E., Tonello, P., Braz Fernandes, F., Vilarinho, P., & Martins, R.

- (2002). Effect of different dopant elements on the properties of ZnO thin films. *Vacuum*, 64(3), 281–285. [https://doi.org/10.1016/S0042-207X\(01\)00322-0](https://doi.org/10.1016/S0042-207X(01)00322-0)
- Orizu, G. E., Ugwuoke, P. E., Asogwa, P. U., & Offiah, S. U. (2023). A review on the inference of doping TiO₂ with metals/non-metals to improve its photocatalytic activities. *IOP Conference Series: Earth and Environmental Science*, 1178(1). <https://doi.org/10.1088/1755-1315/1178/1/012008>
- Prasada Rao, T., Santhosh Kumar, M. C., Safarulla, A., Ganesan, V., Barman, S. R., & Sanjeeviraja, C. (2010). Physical properties of ZnO thin films deposited at various substrate temperatures using spray pyrolysis. *Physica B: Condensed Matter*, 405(9), 2226–2231. <https://doi.org/10.1016/j.physb.2010.02.016>
- Raut, N. C., Mathews, T., Chandramohan, P., Srinivasan, M. P., Dash, S., & Tyagi, A. K. (2011). Effect of temperature on the growth of TiO₂ thin films synthesized by spray pyrolysis: Structural, compositional and optical properties. *Materials Research Bulletin*, 46(11), 2057–2063. <https://doi.org/10.1016/j.materresbull.2011.06.043>
- Shanmuganathan, G., Banu, I. B. S., Krishnan, S., & Ranganathan, B. (2013). Influence of K-doping on the optical properties of ZnO thin films grown by chemical bath deposition method. *Journal of Alloys and Compounds*, 562, 187–193. <https://doi.org/10.1016/j.jallcom.2013.01.184>
- Shinde, S. S., Korade, A. P., Bhosale, C. H., & Rajpure, K. Y. (2013). Influence of tin doping onto structural, morphological, optoelectronic and impedance properties of sprayed ZnO thin films. *Journal of Alloys and Compounds*, 551, 688–693. <https://doi.org/10.1016/j.jallcom.2012.11.057>
- Vijayalakshmi, K., Karthick, K., & Gopalakrishna, D. (2013). Influence of annealing on the structural, optical and photoluminescence properties of ZnO thin films for enhanced H₂ sensing application. *Ceramics International*, 39(5), 4749–4756. <https://doi.org/10.1016/j.ceramint.2012.11.061>
- Vishwas, M., Sharma, S. K., Narasimha Rao, K., Mohan, S., Gowda, K. V. A., & Chakradhar, R. P. S. (2009). Optical, dielectric and morphological studies of sol-gel derived nanocrystalline TiO₂ films. *Spectrochimica Acta Part A: Molecular and Biomolecular Spectroscopy*, 74(3), 839–842. <https://doi.org/10.1016/j.saa.2009.07.018>
- Wang, X., Wu, G., Zhou, B., & Shen, J. (2013). Optical Constants of Crystallized TiO₂ Coatings Prepared by Sol-Gel Process. *Materials (Basel, Switzerland)*, 6(7), 2819–2830. <https://doi.org/10.3390/ma6072819>